A Study on the Influence of Silicon Content on Wear and Mechanical Properties of Cast Nickel-Aluminum Bronze

Chawanan Thongyothee
Department of Industrial Engineering, Faculty of Engineering, King Mongkut's University of Technology Thonburi, Bangkok, Thailand
boby3455@hotmail.com

Sombun Chareonvilisiri
Department of Industrial Engineering, Faculty of Engineering, King Mongkut's University of Technology Thonburi, Bangkok, Thailand
isomsiri@kmutt.ac.th (corresponding author)

Received: 26 August 2024 | Revised: 23 September 2024 | Accepted: 9 October 2024

 DOI: https://doi.org/10.48084/etasr.8817

ABSTRACT

Although aluminum bronze exhibits considerable wear and mechanical properties, nickel-aluminum bronze displays superior performance. A potential issue is the resistance to wear, particularly whether the addition of silicon (Si) enhances anti-wear properties. Samples with varying silicon content (0.2%, 0.4%, and 0.6%) were prepared in three conditions for the purpose of investigating the effects of silicon on wear and mechanical properties. The materials were forged and cast in accordance with the specifications set forth in JIS H 5120 for the production of specimens. The wear and mechanical properties were evaluated through a series of tests, including tensile strength, hardness, impact, and ball-on-disc wear tests. The results demonstrated that, in comparison to ASTM B148-52 or the precursor AlBC-3, as observed in nickel-aluminum bronze, the addition of silicon during the melting of the substrate resulted in a transformation of the precipitation of the kappa phase to $\alpha+\kappa$. The intermetallic compounds were introduced to enhance the formation of pearlite. This resulted in an increase in the tensile strength and hardness of the metal, but a simultaneous decline in its ability to absorb impact. Furthermore, the wear test results indicated that the surface friction coefficient between the nickel-aluminum-bronze disc and the SUS304 stainless steel ball was associated with the amount of silicon added and the hardness. In other words, the workpiece friction coefficient would decrease with increasing hardness due to the rising silicon content. Additionally, it was observed that no adhesive wear was evident between the stainless-steel balls on the nickel-aluminum-bronze disc.

Keywords-cast nickel-aluminum bronze; intermetallic compounds; influence of silicon

I. INTRODUCTION

Copper alloys have a long history of use as friction-reducing materials due to their exceptional combination of properties, including high strength, corrosion resistance, and a naturally slippery surface that effectively minimizes friction. Among these, aluminum bronze, containing 8%-9% aluminum, is the preferred copper alloy for anti-friction applications and environments that demand superior wear resistance. It is employed extensively in components, such as bushings and bearings, where, despite being subjected to relatively low forces, they operate at high rotational speeds. Additionally, aluminum bronze displays noteworthy anti-fatigue characteristics and does not adhere to ductile iron machine parts, thereby making it an optimal choice for such applications [1-3]. The microstructure of aluminum bronze is of great consequence with respect to the determination of its hardness. The incorporation of iron into the alloy results in the refinement of the grain structure, leading to the formation of smaller grains that contribute to an increase in hardness. This grain refinement represents an effective method for enhancing the overall mechanical strength of aluminum bronze. Furthermore, the introduction of iron into the alloy through co-doping with nickel leads to the formation of a kappa (κ) phase within the microstructure. This phase further enhances the hardness of the alloy without compromising its toughness, thereby enabling the material to maintain both strength and durability under mechanical stress [4-6]. Furthermore, the addition of silicon has been observed to exert a strengthening effect on the alloy comparable to that of aluminum. Specifically, 1% by weight of silicon is approximately equivalent to 1.6% by weight of aluminum in terms of its

impact on the alloy's properties. The addition of silicon to aluminum bronze increases the material's hardness, thereby enhancing its wear resistance. This property is particularly beneficial for extending the service life of components subjected to continuous abrasive forces. This includes critical components, such as molds, used in the formation of stainless steel, where prolonged durability is imperative for optimal operational efficiency [6]. During the manufacturing process, nickel-aluminum bronze scrap materials were melted down and silicon was added to the molten alloy. Following alloying, the material was subjected to a series of tests to assess the impact of silicon addition on its mechanical and wear properties. The objective of this process was to identify how the incorporation of silicon could potentially enhance the performance of the recycled alloy [7-10]. Consequently, the objective of the present study was to examine the impact of incorporating silicon in quantities not exceeding 0.6% on the mechanical properties of copper alloys. This approach was designed to enhance the efficiency of producing copper-nickel-aluminum bronze in accordance with the ASTM B148-97 C95800 standard. The objective of the study was to enhance the performance characteristics of the alloy by optimizing the silicon content, thereby improving its overall effectiveness in a range of applications [11]. The results of this study can be used in the engineering and manufacturing industries, particularly in the production of high-performance parts. The optimization of silicon content in copper-nickel-aluminum bronze alloys has the potential to enhance material properties, hence improving the durability and efficiency of components used in demanding applications.

II. EXPERIMENTAL PROCEDURE

This research was carried out through the implementation of an experimental methodology. Specifically, after the molten material was poured into the CO_2 sand mold and allowed to cool, a sample was created that met the specifications set forth in the JIS H 5102 standard [12] for the analysis of various properties, including chemical composition, microstructural examination, mechanical properties, and wear testing. The materials used in the experiments included nickel-aluminum-bronze (AlBC3), commercially pure silicon, and degassing agents to ensure the specimens were free of contamination and free of oil stains and moisture. Additionally, an induction furnace with silicon carbide crucibles was employed. It is essential to achieve the melting point of the metal in a timely manner, and the furnace must possess a high heating rate. Moreover, when melting metal, the application of flux to the surface is essential to prevent the formation of oxides and the absorption of hydrogen. It is important to maintain the furnace atmosphere in a slightly oxidizing state in order to minimize the presence of hydrogen gas [13-16]. It is recommended that the smelting time be kept as short as possible in order to minimize gas dissolution. Furthermore, the prepared materials must be measured according to the calculated amount for each charge, with 30 kg/charge to be melted each time, as shown in Figure 1.

The chemical composition of the samples was examined through the use of an Optical Emission Spectrometer (OES), as presented in Table I. In particular, the sample was subjected to three sparks, and the resulting data were averaged. Once the molten material had been poured into the mold, the specimen was left to cool within the mold. Subsequently, the test specimen was removed from the mold and prepared for further examination and analysis. This involved cutting and shaping the specimen to meet the specifications established in the JIS H5102 standard.

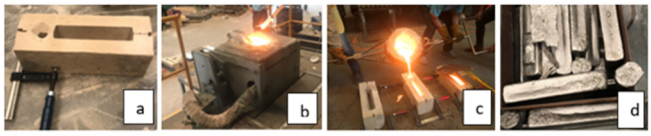

Fig. 1. Casting process (a) prepare the sand mold, (b) Melting and casting, (c) poured into the mold, (d) casting piece.

TABLE I. CHEMICAL COMPOSITION REQUIRED AND OBTAINED BY EMISSION SPECTROMETER ANALYSIS

Materials	Chemical composition (%)					
	Cu	Al	Fe	Ni	Mn	Si
AlBC-3	78.0-85.0	8.5-9.5	3.5-4.5	4.0-5.0	0.8-1.5	0.1 max
0.2% Si	76.57	8.85	3.81	4.16	0.52	0.23
0.4% Si	76.66	8.60	3.59	4.24	0.52	0.46
0.6% Si	77.04	8.40	3.22	4.25	0.52	0.61

The mechanical properties and characteristics of copper-nickel-aluminum-bronze alloys with an adjusted chemical composition were examined. Subsequently, a microstructural examination and wear behavior analysis of the selected samples were conducted using a Scanning Electron Microscope (SEM) [17-19], and Energy Dispersive X-Ray Spectroscopy (EDS). Furthermore, the mechanical properties were investigated, including the tensile strength test (ASTM E8), the Rockwell Hardness test (HRB), and the Charpy Impact test (ASTM E23) [20]. The coefficient of friction was measured through the simple ball-on-disc test in which an austenitic stainless steel (SUS304) ball with a diameter of 6 mm was fixed to a test rod, beam, and weight. The disc was manufactured from nickel-aluminum bronze, with a diameter of 25 mm-30 mm and a thickness of 5 mm-8 mm, in accordance with the ASTM G135-95 standards [8]. The ball-on-disc test was performed in the absence of lubrication, with a load of 10 Newtons, a speed of 10 cm/sec, a radius of 7 mm, and a distance of 800 m, using three specimens per test.

III. RESULTS

A. Results of the Mechanical Properties Test

1) Hardness Testing

The Rockwell hardness B scale was employed to quantify the hardness of nickel-aluminum bronze. Each sample was subjected to three tests, and the mean value was calculated. The results are presented in Table II and Figure 2. The mean hardness value was 77 HRB when silicon was incorporated at concentrations of 0.4% and 0.6% silicon, respectively. It is evident that all three chemical compositions exhibited an increase in hardness when compared to the ASTM B148-52 standard or the AlBC-3 precursor.

TABLE II. RESULTS OF HARDNESS TESTING (HRB)

Materials	Hardness Testing (HRB)
AlBC-3	71
0.2% Si	75
0.4% Si	77
0.6% Si	77

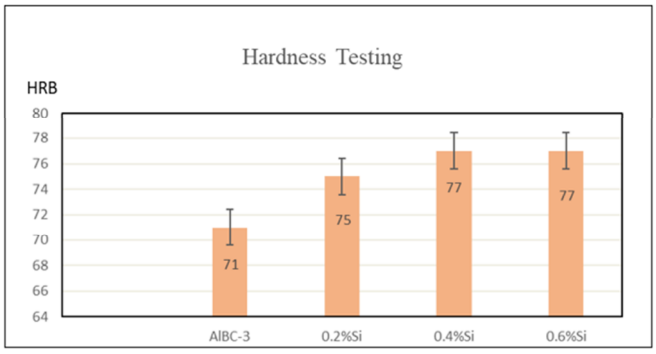

Fig. 2. Hardness test results.

2) Tensile Testing (N/mm2) and Elongation (%)

In order to ascertain the tensile strength in accordance with the ASTM E8 standard, three specimens were prepared and the mean values were calculated, as shown in Table III, Figures 3 and 4.

TABLE III. RESULTS OF TENSILE TESTING (N/MM2) AND ELONGATION (%)

Materials	Tensile Testing (N/mm^2)	Elongation (%)
AlBC-3	588	15
0.2% Si	590	18
0.4% Si	565	12
0.6% Si	594	19

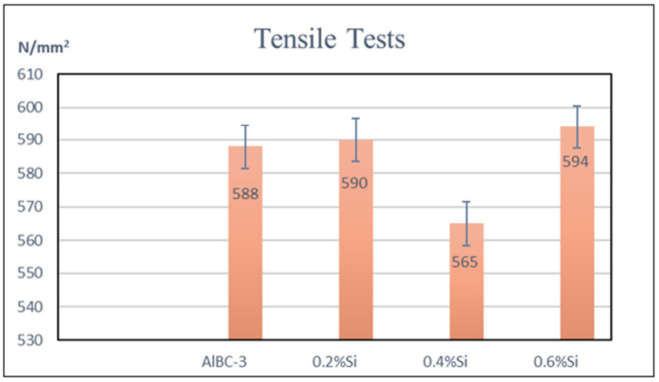

Fig. 3. Results of the tensile test.

As presented in Table III, the test results revealed that the chemical compositions 1 and 3 exhibited elevated tensile strength and elongation percentages when compared to the ultimate tensile strength of nickel aluminum bronze grade C95800, which was cast in accordance with the ASTM B148-52 standard or AlBC-3.

3) Impact Testing

The Charpy impact test was conducted in accordance with the ASTM E23 standard. Three test specimens were created, and the mean values were calculated, as evidenced in Table IV and Figure 5.

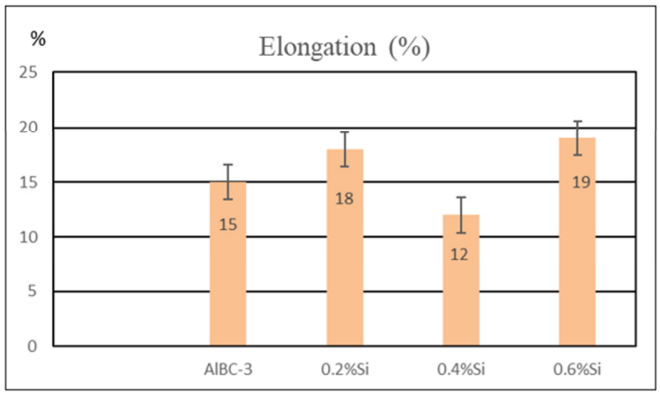

Fig. 4. Results of the elongation (%) test.

TABLE IV. RESULTS OF IMPACT TESTING

Materials	Impact testing (J)
AlBC-3	10
0.2% Si	18
0.4% Si	15
0.6% Si	13

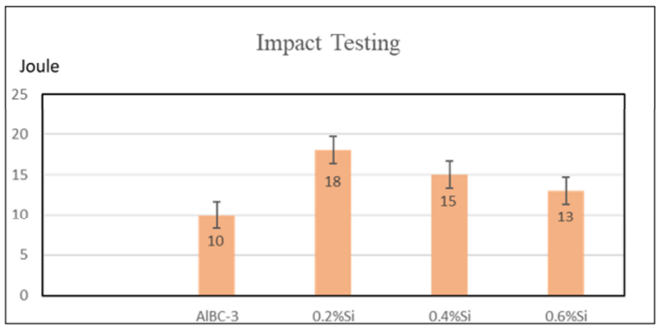

Fig. 5. Results of the impact test.

The Charpy test was used to assess the impact resistance of nickel-aluminum bronze. As portrayed in Table IV, all three compositions exhibited enhanced impact strength relative to the ASTM B148-52 standard and the AlBC-3 precursor. It is noteworthy that the composition containing 0.2% Si exhibited the greatest impact strength, reaching a maximum of 18 J.

B. Results of Wear Testing

1) Coefficient of Friction Testing

In the experiment, a nickel-aluminum-bronze alloy was cast into a plate. A tribological ball-on-disc wear test was performed, in which a SUS304 stainless steel ball was applied with a pressure of 10 N and a linear speed of 10 mm/sec. The data were recorded at regular intervals at a distance of 800 m. The coefficient of friction was determined from the test results using the TriboX.2.9vG program in accordance with the ASSTM G133-95 standard. In particular, the value should be read from the range where the curve is relatively stable. The test results are presented in Table V and Figure 6, with the composition containing 0.6% silicon exhibiting the lowest coefficient of friction among the other compositions.

2) Weight Loss

The tribological ball-on-disc wear test revealed a correlation between the weight loss of the material and the quantity of silicon incorporated. This correlation is shown in Table VI and Figure 7, which depict the relationship between the silicon content and the observed weight loss during the wear test. The composition containing 0.6% silicon demonstrated the lowest weight loss among the other compositions. This suggests that the incorporation of 0.6% silicon resulted in enhanced wear resistance.

TABLE V. COEFFICIENTS OF FRICTION OF THE CONTACTING SURFACES BETWEEN ALUMINUM BRONZE AND SUS304 STAINLESS STEEL

Disc	Friction coefficients (μ)
AlBC-3	0.393
0.2% Si	0.389
0.4% Si	0.343
0.6% Si	0.335

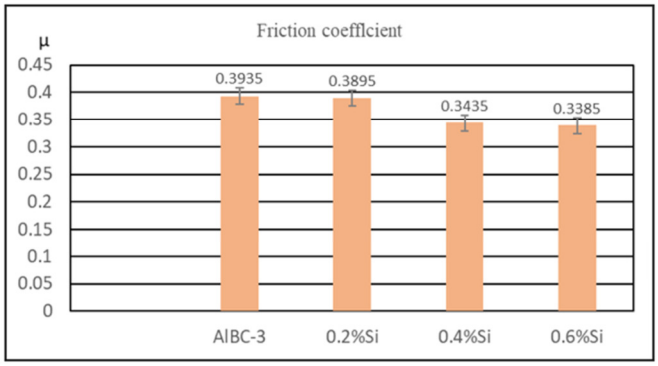

Fig. 6. Coefficient of friction.

TABLE VI. WEIGHT LOSS RELATIVE TO SILICON ADDITION

Materials	Weight Loss (g)
AlBC-3	0.0128
0.2% Si	0.0126
0.4% Si	0.0125
0.6% Si	0.0113

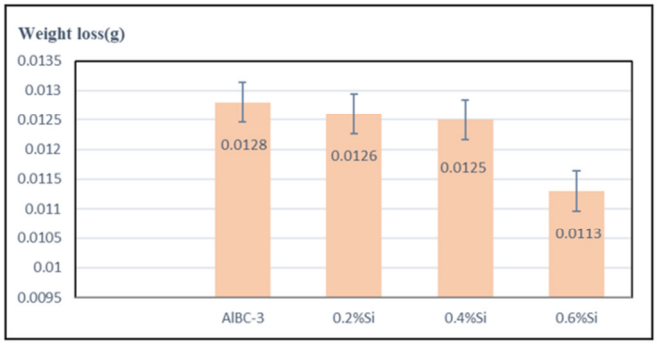

Fig. 7. Relationship between the materials and the weight loss.

The outcomes of the hardness examination for nickel-aluminum bronze are depicted in Table VII. It is evident that all three compositions exhibited an increase in hardness when compared to the ASTM B148-52 standard or the AlBC-3 precursor. The tensile test results demonstrated that the highest tensile strength was 594 N/mm². The tensile strength of composition 2 was found to be inferior to that of C95800 nickel-aluminum bronze cast in accordance with the ASTM B148-52 standard or the AlBC-3 precursor. This is attributed to the fact that the cast specimen in this experiment exhibited porosity, resulting in a discontinuous material structure. Consequently, this resulted in a reduction in strength. The Charpy impact test for nickel-aluminum bronze demonstrated that all three compositions displayed enhanced impact strength in comparison to the ASTM B148-52 standard or the AlBC-3 precursor. In particular, the first composition achieved a maximum impact strength of 18 joules. However, an increase in the amount of silicon results in a corresponding decrease in impact strength [21-23]. The coefficient of friction of the contacting surfaces between aluminum bronze and stainless steel SUS304 can be determined from the test results using TriboX.2.9G in accordance with the ASTM G133-95 standard. The values should be read from the range where the curve is relatively stable. Among the other compositions, the third, which contains 0.6% silicon, exhibited the lowest coefficient of friction. After the test, the discs were analyzed for wear marks using a light microscope at 50x magnification at a distance of 800 meters, as shown in Figure 8.

TABLE VII. MECHANICAL PROPERTIES AND WEAR TESTS

Material	Tensile Testing (N/mm^2)	Impact Testing (J)	Hardness Testing (HRB)	Friction Coefficient	Weight Loss (g)
AlBC-3	588	10	71	0.3935	0.0128
0.2% Si	590	18	75	0.3895	0.0126
0.4% Si	565	15	77	0.3435	0.0125
0.6% Si	594	13	77	0.3385	0.0113

The findings indicated that an elevated silicon concentration led to a reduction in the width of the observed wear marks. The resulting wear appeared as sliding and permanent deformation. As a result, the groove's smooth surface became uneven, leading to a loss of friction and, consequently, shearing on the surface. As illustrated in Figure 8, the wear groove exhibited a pronounced width in comparison to other compositions. The deformation of the material, which can be attributed to shear forces exerted by the indenter on the specimen, is permanent. However, the elevated wear rate resulted in a distinct coefficient of friction. This is due to the fact that the increased speed and weight cause severe and rapid wear on the specimen. This phenomenon causes the formation of surface pullouts due to fatigue resulting from the repeated application of pressure. Additionally, wear caused by abrasion, results from particles being pulled out of the wear groove and subsequently pushed along the groove, leading to an increase in the shearing of the material. It can be thus concluded that the rotational speed and load exerted had an effect on the wear rate observed on the surface of the specimen in the dry-slide wear test. In the event that the scales are not sufficiently precise or the weighing procedures are not meticulously followed, the results of the weight loss will exhibit minimal discrepancies. This can lead to difficulties in distinguishing weight variations, resulting in the unnecessary expenditure of time during the testing process [24-26]. As

shown in Figure 8, the silicon-added cast nickel-aluminum-bronze discs demonstrated a tendency to exhibit less weight loss than other compositions. Furthermore, discs with lower hardness are less resistant to wear, resulting in greater weight loss.

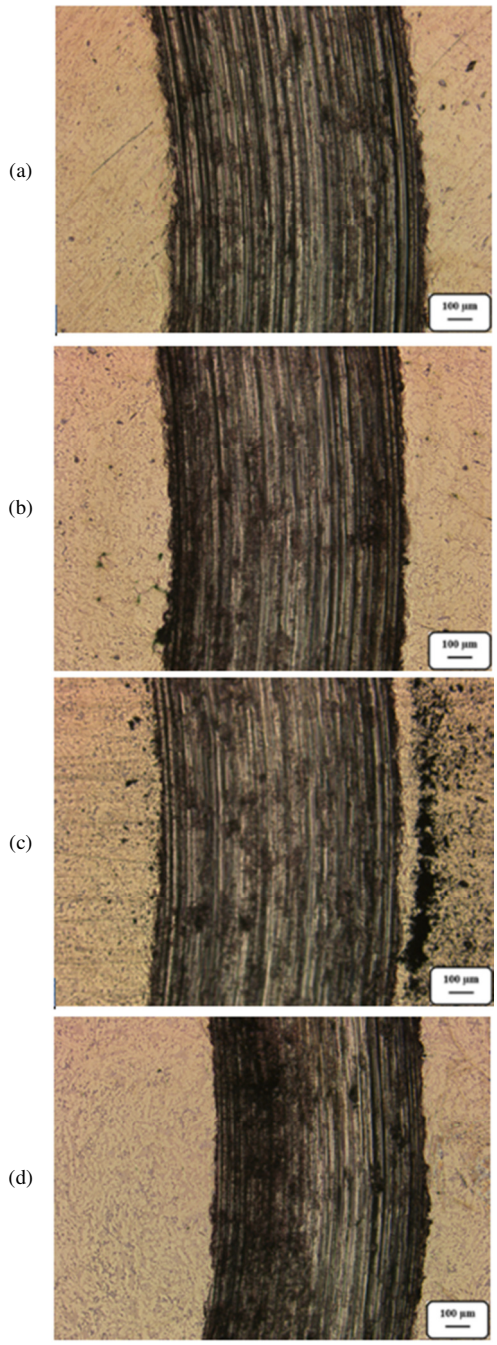

Fig. 8. Wear marks at a distance of 800m and 50x magnification across all compositions (a) AlBC-3, (b) 0.2%Si, (c) 0.4%Si, (d) 0.6%Si.

C. Microstructure

During the cooling phase transformation of the nickel-aluminum-bronze alloy [27-29], which occurs at temperatures below 460 °C, the solubility of iron and silicon allows for the formation of nuclei, which subsequently grow as the spherical precipitated phase, namely the intermetallic k_{IV} phase, which is rich in iron and other alloying elements. The precipitation pattern of the k_{IV} phase may be attributed to its formation at relatively low temperatures, and the diffusion of the mixture within the α phase may occur over relatively short distances following rapid cooling. The remaining $\beta(\beta(\text{Al}))$ phase, which does not undergo conversion to the α phase due to its high Al content, undergoes transformation into the $\alpha+\gamma_2$ eutectoid through primary and secondary crystallization. The solid transition phase in the microstructure is formed by the microstructure of the phase, which consists of the following phases: $k_{II} + (\alpha+k_{III}) + (\alpha+k_{IV}) + (\alpha+\gamma_2)$ [30-38], where γ_2 is used instead of β'. All the previously mentioned results, are presented in Figures 9-12.

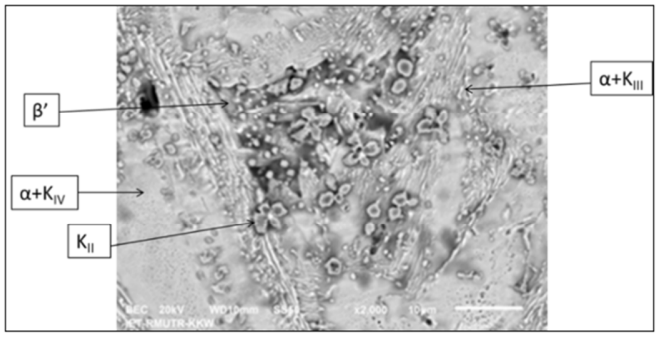

Fig. 9. Microstructure of nickel aluminum bronze, at 2000X magnification.

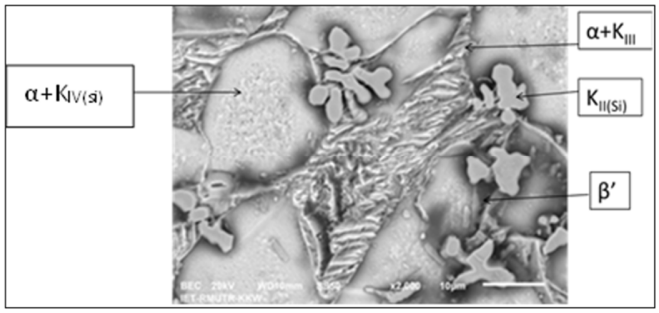

Fig. 10. Microstructure of 0.2% Si-added nickel aluminum bronze at 2000X magnification.

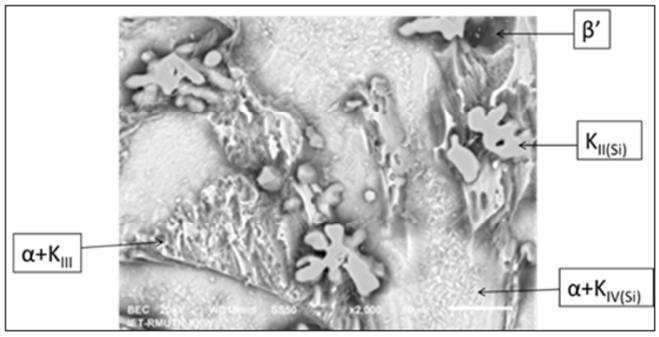

Fig. 11. Microstructure of 0.4% Si-added nickel aluminum bronze at 2000X magnification.

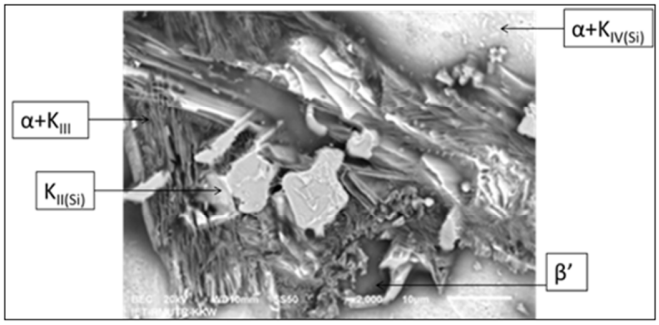

Fig. 12. Microstructure of 0.6% Si-added nickel aluminum bronze filled at 2000X magnification.

A comparative analysis of the microstructures revealed that the addition of silicon to the nickel-aluminum-bronze casting alloy resulted in the formation of the iron k_{II}(Si) complex, accompanied by the precipitation of k_{IV}(Si) in minor quantities during the cooling process. This resulted in the inhibition of α-phase growth, which led to a reduction in its dimensions in comparison to those observed in nickel-aluminum-bronze alloys that did not contain silicon. Upon increasing the quantity of silicon, it was observed that the microstructure manifested as a metal compound structure (intermetallic compound; CuAl, NiAl), bearing resemblance to the lamellar pearlite of carbon steel. This structure is notable for its high hardness but is also brittle and fragile [20, 28, 29, 38-40]. To ensure the clarity of the microstructure, the elemental content of phases was analyzed through the EDS technique across all four compositions of nickel-aluminum-bronze casting specimens. It was observed that the gray, round particles exhibited a higher iron content than other areas. This suggests the presence of a k_{II} phase, which is an intermetallic compound comprising Fe_3Al constituents. This phase displays high hardness and exhibits morphological features characteristic of a rosette shape. The k_{III} phase is distinguished by a lamellar structure comprising NiAl constituents. The fine globular particles are identified as the k_{IV} phase, composed of Fe3Al constituents, as presented in Figures 13-16.

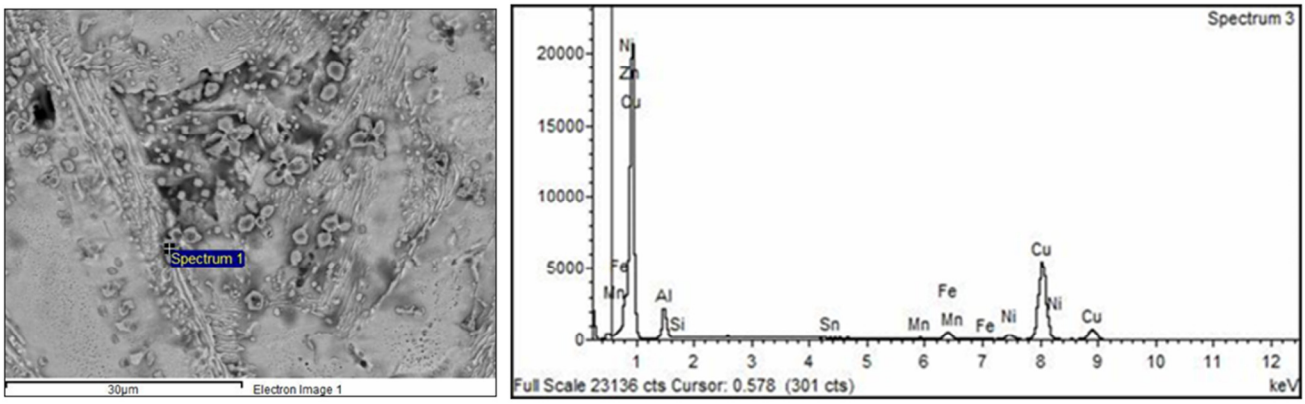

Fig. 13. Elemental analysis of phases of nickel-aluminum-bronze casting alloys using the EDS technique.

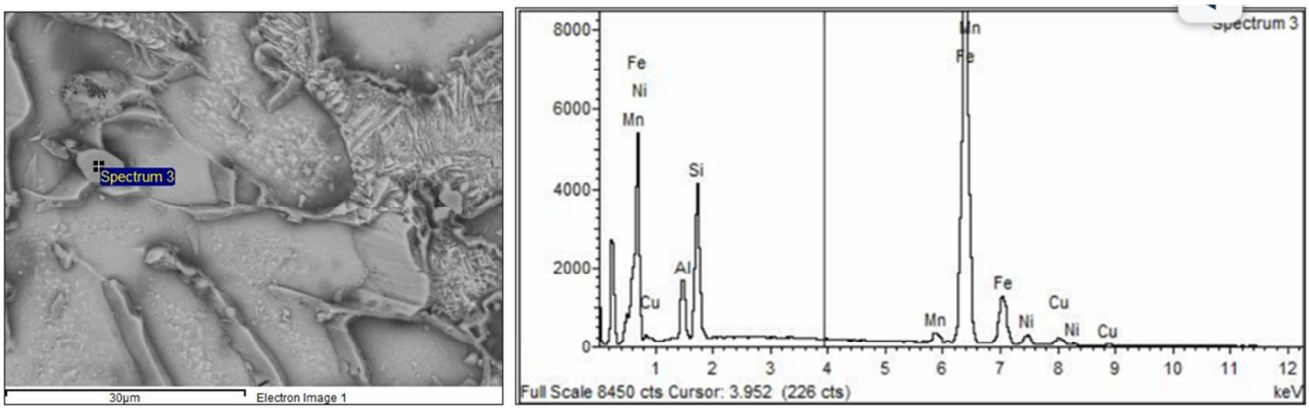

Fig. 14. Elemental analysis of the phase with 0.2% silicon through the EDS technique.

IV. CONCLUSIONS

The results of this experiment clearly demonstrated that the addition of silicon had a significant impact on both the wear behavior and the mechanical properties of nickel-aluminum bronze castings. The results of this experiment can be summarized as:

- The incorporation of silicon into the nickel-aluminum bronze casting alloy at varying concentrations of 0.2%,

0.4%, and 0.6% was found to result in a notable increase in both tensile strength and hardness. It is important to note, however, that while these properties improved, the impact strength exhibited a declining trend when the silicon content surpassed 0.6%. This indicates that excessive silicon may compromise the alloy's ability to withstand sudden or shock loading.

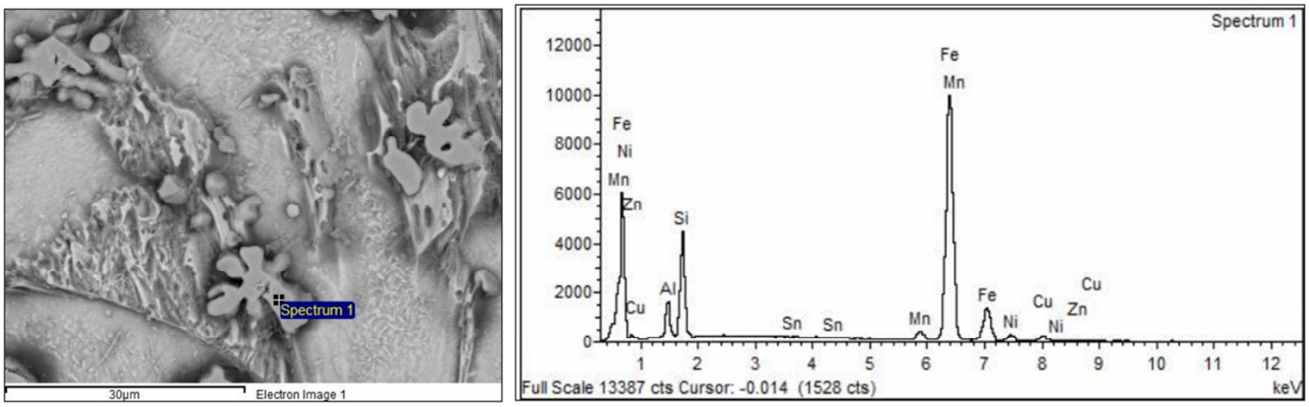

Fig. 15. Elemental analysis of the phase with 0.4% silicon added through the EDS technique.

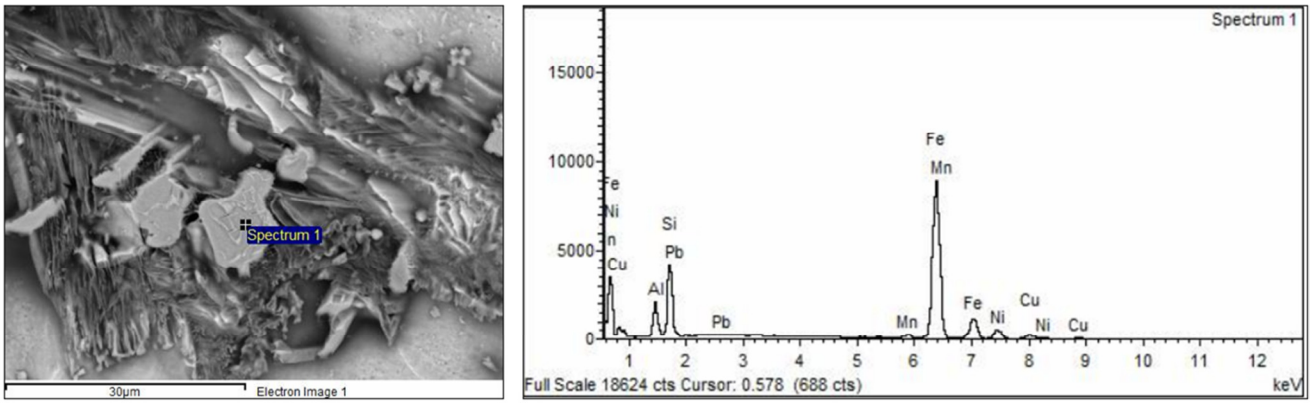

Fig. 16. Elemental analysis of the phase with 0.6% silicon doping through the EDS technique.

- Furthermore, the incorporation of silicon into the nickel-aluminum bronze casting alloy was found to be a critical factor in reducing the wear rate. The wear groove characteristics observed on the surface of the specimen were indicative of a wear mechanism driven by the repeated application of pressure and shear forces exerted by the indenter on the workpiece surface. This interaction resulted in the localized loss of material in specific areas. It is noteworthy that when the silicon content reached 0.6%, the wear on the alloy was significantly less severe compared to alloys with 0.2% and 0.4% silicon. This can be attributed to the enhanced hardness associated with higher silicon content. It can be therefore concluded that the silicon content exerts a direct and quantifiable influence on the wear resistance of the nickel-aluminum bronze casting alloy.
- In terms of hardness, the silicon-modified nickel-aluminum bronze alloy exhibited superior performance in comparison to 304-grade stainless steel, which typically has a hardness of approximately 240 HB. Additionally, the findings of the wear test demonstrated the absence of evidence suggestive of adhesive wear between the stainless steel and the nickel-aluminum bronze alloy that had been enhanced with silicon. Moreover, the coefficient of friction between the nickel-aluminum bronze alloy and stainless steel was found to be lower than that observed between the original, unmodified nickel-aluminum bronze alloy and stainless steel after testing for a sliding distance of 800 meters. This suggests that the presence of silicon has resulted in improved wear characteristics.
- The microstructural analysis demonstrated that the incorporation of silicon into the copper-nickel-aluminum casting alloy resulted in substantial alterations to its phase structure. Specifically, silicon was found to bind to the α phase, while also altering the k phase, which resulted in a reduction in the size of the α phase and a more dispersed distribution within the k phase. This, in turn, impeded the expansion of the α phase, leading to a more refined grain structure and, consequently, enhanced mechanical properties across the alloy.

This research makes a significant contribution to both the theoretical and practical aspects of materials science, providing

a comprehensive understanding of the influence of silicon on the properties of nickel-aluminum bronze. The findings of this study are expected to inform future alloy development and enhance the performance of materials used in demanding applications.

ACKNOWLEDGMENT

The research was carried out in the Department of Industrial Engineering. Faculty of Engineering, King Mongkut's University of Technology Thonburi. The authors are deeply grateful to Mr. Chaow Niamson president of PCS Foundry Products Co., Ltd. for their invaluable advice, and to the financial support of this research project.

REFERENCES

[1] E. G. West, *Copper and Its Alloys*. Chichester, UK: E. Horwood, 1982.

[2] A. F. Society, *Casting Copper-Base Alloys*, 1st ed. Illinois, USA: American Foundrymen's Society, 1984.

[3] W. D. Callister, *Fundamentals of Materials Science and Engineering*, 2nd ed. Hoboken, NJ, USA: Wiley, 2004.

[4] I. Richardson and O. Gouriou, "Nickel Aluminium Bronze: a reconsideration for valve manufacture," *Valve World*, pp. 1–4, Oct. 2017.

[5] I. Richardson, *Guide to nickel aluminum bronze for engineers*. Hertfordshire, UK: Copper Development Association, 2016.

[6] H. Meigh, Cast and Wrought Aluminium Bronzes: Properties, Processes and Structure, 1 st. London, UK: CRC Press, 2000.

[7] J. H. D. Bautista, "Aluminum bronze," *Metal Casting Technologies*, vol. 51, no. 4, pp. 38–40, 2012.

[8] J. H. D. Bautista, "Metal for a virtual bronze foundry," *Metal Casting Technologies*, vol. 58, no. 1, pp. 38–42, 2012.

[9] J. H. D. Bautista, "Raw materials for the virtual bronze foundry," *Metal Casting Technologies*, vol. 59, no. 1, pp. 37–40, 2013.

[10] J. H. D. Bautista, "Chemical and physical testing of bronze castings," *Metal Casting Technologies*, vol. 58, no. 2, 2013, Art. no. 34.

[11] *ASTM B148-18 Standard specification for aluminum bronze sand casting*. West Conshohocken, PA, USA: ASTM International, 2018.

[12] *JIS handbook: non-ferrous metals & metallurgy*, 1st ed. Tokyo, Japan: Japanese Standards Association, 1996.

[13] *ASM Handbook: Casting*, 9th ed. Ohio, USA: ASM International, 1988.

[14] M. Sahoo and S. Sahu, *Principles of Metal Casting, Third Edition*, 3rd edition. New York, USA: McGraw Hill, 2014.

[15] J. F. Meredith, "Solidification and feeding of copper-base castings," *Metal Casting Technologies*, vol. 52, no. 4, pp. 44–46, 2006.

[16] J. F. Meredith, "Casting of copper-base casting," *Metal Casting Technologies*, vol. 53, no. 4, pp. 58–60, 2007.

[17] A. W. El-Morsy, "Wear Analysis of a Ti-5Al-3V-2.5Fe Alloy Using a Factorial Design Approach and Fractal Geometry," *Engineering, Technology & Applied Science Research*, vol. 8, no. 1, pp. 2379–2384, Feb. 2018, https://doi.org/10.48084/etasr.1743.

[18] O. Bildik and M. Yaşar, "Manufacturing of Wear Resistant Iron-Steel: A Theoretical and Experimental Research on Wear Behavior," *Engineering, Technology & Applied Science Research*, vol. 11, no. 3, pp. 7251–7256, Jun. 2021, https://doi.org/10.48084/etasr.4092.

[19] E. R. I. Mahmoud and H. F. El-Labban, "Microstructure and Wear Behavior of TiC Coating Deposited on Spheroidized Graphite Cast Iron Using Laser Surfacing," *Engineering, Technology & Applied Science Research*, vol. 4, no. 5, pp. 696–701, Oct. 2014, https://doi.org/10.48084/etasr.483.

[20] K. S. Abdel-Wahab, A. Hussein, E. M. E. Banna, and M. Waly, "Effect of chromium and silicon additions on the microstructure and mechanical properties of complex aluminum bronze," *International Journal of Metallurgical & Materials Science and Engineering*, pp. 18–27, 2015.

[21] G. Adeyemi, B. S. Oluwadare, and K. O. Olanipekun, "Investigation on the effect of addition of magnesium on the microstructure and mechanical properties of aluminum bronze," *International Journal of Engineering Science Invention*, vol. 2, no. 11, pp. 1–13, Nov. 2013.

[22] A. A. Imah, S. C. Ekenyem, C. C. Ogbu, G. O. Ewa, and E. E. Nnuka, "Effect of nickel addition on the structure and mechanical properties of aluminium bronze (cu-10%al) alloy," *International Journal of Engineering Inventions*, vol. 9, no. 1, pp. 41–51, Jan. 2020.

[23] C. N. Nwambu, I. M. Anyaeche, G. C. Onwubiko, and E. E. Nnuka, "Modification of the structure and mechanical properties of aluminum bronze (Cu-10%Al) alloy with Zirconium and Titanium," *International Journal of Scientific & Engineering Research*, vol. 8, no. 1, pp. 1048–1057, Jan. 2017.

[24] M. Moradlou, N. Arab, R. Emadi, and M. Meratian, "Effect of magnesium and nickel on the wear and mechanical properties of casting bronzes," *Journal of American Science*, vol. 7, no. 7, pp. 717–722, 2011.

[25] R. J. Bayer, *Mechanical Wear Fundamentals and Testing, Revised and Expanded*, 2nd ed. Boca Raton, Fl, USA: CRC Press, 1994.

[26] K. G. Budinski, *Mnl 56 Guide to Friction, Wear and Erosion Testing*. West Conshohocken, PA, USA: ASTM International, 2007.

[27] G. W. Stachowiak, *Wear: Materials, Mechanisms and Practice*. Chichester, UK: John Wiley & Sons, 2006.

[28] J. Miettinen, "Thermodynamic description of the Cu–Al–Si system in the copper-rich corner," *Computer Coupling of Phase Diagrams and Thermochemistry*, vol. 31, no. 4, pp. 449–456, Dec. 2007, https://doi.org/10.1016/j.calphad.2007.05.001.

[29] S. M. Orzolek, J. K. Semple, and C. R. Fisher, "Influence of processing on the microstructure of nickel aluminum bronze (NAB)," *Additive Manufacturing*, vol. 56, Aug. 2022, Art. no. 102859, https://doi.org/10.1016/j.addma.2022.102859.

[30] P. R. Howell, "On the phases, microconstituents and microstructures in nickel–aluminum bronzes," Copper Development Association Inc., Technical, 2000.

[31] B. Pisarek, "The crystallisation of the aluminium bronze with additions of Si, Cr, Mo and/or W," *Archives of Materials Science and Engineering*, vol. 28, pp. 461–466, Aug. 2007.

[32] B. Pisarek, "Model of Cu-Al-Fe-Ni Bronze Crystallization," *Archives of Foundry Engineering*, vol. 14, no. 4, pp. 39–44, Jun. 2013, https://doi.org/10.2478/afe-2013-0063.

[33] E. A. Feest and I. A. Cook, "Pre-primary phase formation in solidification of nickel-aluminium bronze," *Metals Technology*, vol. 10, no. 1, pp. 121–124, Jan. 1983, https://doi.org/10.1179/030716983803291802.

[34] F. Hasan, J. Iqbal, and N. Ridley, "Microstructure of as-cast aluminium bronze containing iron," *Materials Science and Technology*, vol. 1, no. 4, pp. 312–315, Apr. 1985, https://doi.org/10.1179/mst.1985.1.4.312.

[35] E. A. Culpan and G. Rose, "Microstructural characterization of cast nickel aluminium bronze," *Journal of Materials Science*, vol. 13, no. 8, pp. 1647–1657, Aug. 1978, https://doi.org/10.1007/BF00548728.

[36] F. Hasan, A. Jahanafrooz, G. W. Lorimer, and N. Ridley, "The morphology, crystallography, and chemistry of phases in as-cast nickel-aluminum bronze," *Metallurgical Transactions A*, vol. 13, no. 8, pp. 1337–1345, Aug. 1982, https://doi.org/10.1007/BF02642870.

[37] R. Thomson and J. O. Edmunds, "The kappa phase in nickel-aluminum bronze, part 2: Cast microstructures & properties," *Transactions of the American Foundrymen's Society*, 1978.

[38] A. Jahanafrooz, F. Hasan, G. W. Lorimer, and N. Ridley, "Microstructural development in complex nickel-aluminum bronzes," *Metallurgical Transactions A*, vol. 14, no. 10, pp. 1951–1956, Oct. 1983, https://doi.org/10.1007/BF02662362.

[39] J. Iqbal, F. Ahmed, and F. Hasan, "Development of Microstructure in Silicon-Aluminum-Bronze," *Pakistan Journal of Engineering and Applied Sciences*, vol. 3, pp. 47–53, Jul. 2008.

[40] M. Sadayappan, F. A. Fasoyinu, R. Zavadil, and M. Sahoo, "Effect of some impurity elements on the mechanical properties of aluminum bronze alloys C95800 and C95400," *Transactions of the American Foundrymen's Society*, vol. 106, pp. 743–748, 1998.